The Study on the Impact of ATM Gene Silencing on Hela Cell Radiosusceptibility

LUO Judong [1, 2, #], GE Yangyang [2, #], ZHOU Xifa *, [1], LU Xujing [1], ZHANG Shuyu [2], TANG Hua [1], LING Yang [1], CHEN Ling [1], CAO Jianping *, [2]

[1] Changzhou Tumor Hospital, Soochow University, Changzhou, 213001, China
[2] School of Radiation Medicine and Protection; Jiangsu Provincial Key Laboratory of Radiation Medicine and Protection, Soochow University, Suzhou 215123, China

ABSTRACT

Objective By using conventional chromosome aberration analysis, the radiosensitivity of Hela cells by silencing ATM gene (Hela^{ATM-} cell) using siRNA technology was investigated.

Methods (1) ATM siRNAs were designed and synthesized, including four pairs of siRNAs specifically targeting ATM gene, a negative control siRNA and a FAM-marked siRNA as a negative control. Transfections of these siRNAs into Hela cells were performed using liposome, transfection efficiency was monitored under fluorescent microscope. ATM expression of transfected Hela cells was detected at different time by using RT-PCR assays. (2) By using conventional chromosome aberration analysis method, chromosome aberration frequencies (CAF) of Hela^{ATM-} cells and Hela cells exposed to ^{60}Co γ-ray were observed compared to control Hela cells.

Results (1) FAM-marked negative control siRNA was successfully transfected into Hela cells as monitored by fluorescent microscope. (2) The data with RT-PCR assays showed that ATM gene expression was significantly depressed in Hela^{1057} cells (transfection with 1057-1075nt siRNA) 24h following transfection ($p<0.05$). The 1057-1075nt siRNA worked until 96h after transfected ($p<0.05$). ATM gene expression was decreased significantly at 24h and 48h after transfected compared to 96h ($p<0.05$), no significant difference between 24h and 48h, 72h and 96h after transfected ($p>0.05$); ATM gene expression was decreased significantly at 24h and 48h than 72h and 96h after transfection ($p<0.05$). (3) After exposed to 0, 1, 2, 3, 4 and 5 Gy ^{60}Co γ-ray, the main pattern of chromosome aberration was dic and the radiation-induced level of CAF was significantly higher in Hela^{ATM-} cells than in control Hela cells at each dose point ($p<0.01$). In the two cells, CAF had a positive correlation with the doses used, and their linear regression equation was $Y=a+bD$. The slope of CAF linear regression equations of Hela^{ATM-} cells was larger than that of control Hela cells ($p<0.05$).

Conclusion (1) ATM gene was successfully silenced by transfection of chemically synthesized siRNAs in Hela cells, named Hela^{ATM-}. (2) The CAF of Hela^{ATM-} cells was significantly higher than control Hela cells by using conventional chromosome aberration analysis.

Key Words

RNAi, ATM, Radiosensitivity, Conventional chromosome aberration analysis method.

Correspondence to:

ZHOU Xifa, CAO Jianping

E-mail: lhpljd@yahoo.com.cn

The first two authors[#] contributed equally to this work.

The gene mapping of ATM (ataxia telangiectasia mutated, ATM) is located on human chromosome 11q22-23, and its total length is about 150Kb, with a coded sequence around 12Kb. 3056 amino acids consists of the protein, and the relative molecular weight is about 350 KDa. ATM contains the Wortmannin-inhibited Ser/Thr protein kinase active site, thus belonging to the PI-3K (phosphatidylinositol 3-kinase) kinase family [1]. When factors such as ionizing radiation generate DNA damages, the dominant kinase ATM can be initiated and directly feel DNA double-stranded breaking (DSB) damage signals, which can catalyze the phosphorylation of a variety of important functional substrate proteins, participate in cell cycle regulation, DNA damage signal transduction and the repair of DNA damage, and maintaining the chromosomal stability. Thus, ATM is the hub of the cell response signal transduction pathway [2]. However, whether ATM expression is associated with chromosome aberration is still unknown.

RNA interference (RNAi) indicates that the introduction of endogenic and ectogenic double strand RNA (double-stranded RNA, dsRNA) into cells of organisms, which generate the the degradation of homologous mRNA specificity, and the later post-transcripitional gene silencing (PTGS) [3,4]. For small interfering RNA (siRNA) with a length of 21-23nt, they are key intermediate effector molecules of RNAi. siRNA applies sequence specificity to inhibit target gene expressions, and its high efficiency and high specificity

LUO Judong, GE Yangyang, ZHOU Xifa, LU Xujing, ZHANG Shuyu, TANG Hua, LING Yang, CHEN Ling, CAO Jianping. The study on the impact of ATM gene silencing on Hela cell radiosusceptibility. Science and Nature (2013) 2(1):35-40. (ISSN 2324-7290) © ZolCat Academic House. www.zolcat.com

demonstrate outstanding advantages in the study of gene function and gene therapy [5,6].

According to the design principles of Tuschl T siRNA [7], siRNA on ATM gene was designed and synthetized to transfect tumor cells and observe the gene silencing effects. This can provide models for the research into biological characteristics of the tumor cells with ATM afunction. The conventional chromosome aberration analysis method was adopted to study on its radiosusceptibility, and provided theoretical and experimental basis for further research on how to improve tumor radiosusceptibility.

1 Materials and Methods

1.1 Materials

Hela cervical cancer cells (Shanghai Cell Bank, Chinese Academy of Sciences); DMEM medium and newborn calf serum (Invitrogen); RNeasy Mini Kit (QIAGEN); QIAshredder Homogenizers (QIAGEN); Lipofectamine^{TM}2000 (Invitrogen); One Step RT-PCR Kit (TaKaRa); 4 pairs of siRNA, positive and negative control siRNA (Shanghai Jima Company); PCR primers: ATM gene primer, GAPDH primers , β-actin primers (Shanghai Sangon); colchicine, Giemsa (Sigma).

1.2 Methods

1.2.1 Design and Synthesis of siRNA Sequences

According to the design principle of siRNA, four pairs of siRNA were designed and synthesized for ATM mRNA (NM_000051), as well as one pair of negative control siRNA NC, one pair of positive control siRNA PC (for GAPDH mRNA and NM_002046). In addition, one pair of negative control FAM-NC of marked FAM was synthesized for the observation of the observed effects under a fluorescent microscope. All siRNAs were synthesized by Shanghai Jima Company. Each sequence is shown in Table 1.

1.2.2 Cells Transfection

Hela cells were seeded in DMEM medium supplemented with 10% fetal bovine serum for serial subcultivation in the incubator with 5% CO_2 at 37°C, and the passage number <20. 24h before transfection, (1-3)×10^5 Hela cells were seeded in 6-pore plates, so that the cell density in the transfection can reach 30-70%. In the transfection, the serum-free DMEM medium was replaced. According to 5ul Lipofectamine^{TM}2000 per pore: 150pmol siRNA was used to transfect Hela cells (refer to the operations on the manual). 5h after the transfection, DMEM medium supplemented with 10% fetal bovine serum was replaced. The above experiments were divided into 5 groups: A. 4 pairs of transfected ATM siRNA; B. positive control siRNA transfected PC group; C. negative control siRNA transfected NC group; D. normal Hela cells; E. FAM-NC negative control transfected group. Cells of each group were named after the transfected siRNA sequence, such as the transfected Hela cells of 1057-1075nt siRNA were named as Hela^{1057}, and cells with interference effects were named as Hela^{ATM-} cells.

1.2.3 the transfection efficiency of the cells of the group E observed under the fluorescence microscope

1.2.4 One Step RT-PCR

RNeasy Mini Kit was used to extract the total mRNA of cells in each group. OD values were measured with a nucleic acid UV spectrophotometer, with A260/A280 of 1.8~2.1 for ATM mRNA expression 24h after the A, C, D cells transfected siRNA. The primer design was completed with Primer Premier5.0, and synthesized with GenBank Blast analysis. β-actin mRNA (NM_001101) was selected as the internal standard to identify the relative expression mRNA level of ATM gene.

(1) Sequences are as follows:

ATM Primer Sequence:

Forward Primer: 5'-GCATTACGGGTGTTGAAGGTGTC-3'
Reverse Primer: 3'-AGAAACTGACCTGGTACTTAGGAA-5'

β-actin Primer Sequence :

Forward Primer: 5'-ACGACCCATTCGAACGTCTG-3'
Reverse Primer: 3'-CTCCCTCGGACTCTTTGCC-5'

(2) The reverse-transcription reaction system:

Hela mRNA	A or B or C or D Group'	0.1ug
ATM or β-actin or GAPDH	Forward Primer (20uM)	0.2ul
	Reverse Primer (20uM)	0.2ul
2×One Step RT-PCR Buffer		12.5ul
TaKaRa EX Taq HS (5U/ul)		0.5ul
M-MLV RTase(Rnase H free,200U/ul)		0.25ul
RNase Inhibitor(40U/ul)		0.5ul
RNase Free dH_2O	Supplmentary 25ul system	

(3) The PCR conditions:

ATM: RT: 42°C 15min, 95°C 2min, PCR: 95°C 5s , 60°C 20s , 72°C 15s , 28 cycles.

β-actin: RT: 42°C 15min, 95°C 2min , PCR: 95°C 5s , 56°C 20s , 72°C 15s , 28 cycles.

Table 1. Designed siRNA sequences

No.	Corresponding Location on mRNA	Nucleotide Sequence	GC Content (%)
1	1057-1075nt	Sense 5'-GAGCUCUUCAGGUCUAAAUdTdT-3' Antisense 5'-AUUUAGACCUGAAGAGCUCdTdT-3'	39.0
2	4661-4679nt	Sense 5'-GCAGCUGAAACAAAUAAUGdTdT-3' Antisense 5'-CAUUAUUUGUUUCAGCUGCdTdT-3'	33.3
3	5746-5764nt	Sense 5'-AGGCCUGGAUGAUAUAAAUdTdT-3' Antisense 5'-AUUUAUAUCAUCCAGGCCUdTdT-3'	33.3
4	7192-7210nt	Sense 5'-GCUCCCUGAAAGGGCAAUAdTdT-3' Antisense 5'-UAUUGCCCUUUCAGGGAGCdTdT-3'	47.6
5	negative control NC	Sense 5'-UUCUCCGAACGUGUCACGUTT-3' Antisense 5'-ACGUGACACGUUCGGAGAATT-3'	47.6
6	positive control PC	Antisense 5'-AUUUAGACCUGAAGAGCUCdTdT-3' Antisense 5'-CUUGAGGCUGUUGUCAUACTT-3'	42.8

(4) The product analysis:

The PCR products were treated with 1.5% agarose gel electrophoresis, photoed with the ultraviolet image analyzer and semi-quantitative analysis with Bandscan5.0 Gel Image Analysis Software. The relative expression level of Hela cell ATM mRNA =ATM cDNA/ β-actin cDNA. ATM amplification product is 138bp and β-actin amplification product is 564bp.

1.2.5 Ionizing Radiation

At room temperature, ^{60}Coγ ray was used to irradiate Hela cells and Hela^{ATM-} cell (24h after the transfection of siRNA) in the logarithmic phase, and the adsorbed dose is 0, 1, 2, 3, 4, and 5Gy (dosage rate as 1.0Gy/min). After the ^{60}Coγ ray irradiation, the medium was repalced immediately and added with colchicine (with the final concentration as 0.10μg/ml), and the medium was cultured for another 24h.

1.2.6 The Preparation of Chromosome Specimens

0.25% trypsin was used to harvest cells, which were then removed in a centrifuge tube, treated with centrifugation at 1,500r/min for 8min. The upper layer of medium was removed and cells were harvested with centrifugation. The cells were treated with low permeability of 0.075M KCl and fixed with fresh fixative (methanol: ice acetic acid = 3:1), conventional droplet sheet and Giemsa staining, eventually producing the chromosome fragments.

1.2.7 Chromosome Aberration Analysis

Metaphase with sound chromosomes dispersity was selected under the microscope, and various chromosomal aberration types were counted, mainly including dicentric mitochondrial (dic) and centromere ring (r). The blind reading was adopted so that the distortion seen by an observer must be reviewed by another observer.

1.2.8 Statistical Analysis

The statistical software of SPSS13.0 for windows was adopted. The RT-PCR experimental data was expressed by mean ± standard deviation. The relationship between chromosome aberration rate and dose of Hela cells and Hela$^{ATM—}$ cell was treated with linear correlation analysis. Meanwhile, the distortion rate of each dose point between two cells was compared with One-Way ANOVA.

2 Result

2.1 Observation of the efficiency of the cells transfected with the siRNA

The transfection efficiency of cells after the transfection of siRNA was observed under an inverted fluorescence microscope. A, B are photos under an ordinary microscope, and C is the photo under a fluorescence microscope. With the comparison of three groups, it can be observed that in A, there is no bright spot in Hela cells with high refractive index; in B, there are bright spots in Hela^{1057} with high refractive index, as the mixation of Lipofectamine^{TM}2000 and siRNA; in C, the green fluorescent in cells is simulated and initiated by FAM, consistent with bright spots in cells in B, indicating that Lipofectamine^{TM}2000 successfully mediated siRNA- transfected Hela cells (as shown in Figure 1).

2.2 Interference Effect Screening of siRNA Inhibition of ATM Gene

At 24h of the siRNA transfection of Hela cells, β-actin and ATM mRNA expressions are shown in Figure 2A. The relative expression quantity of ATM mRNA in cells is shown in Table 2 and Figure 2B. At 24h, 48h, 72h, 96h of 1057-1075nt siRNA transfection of Hela^{1057} cells, RT-PCR results of ATM and β-actin are shown in Figure 3A, and the relative expression of ATM mRNA is shown in Figure 3B.

As shown in Figure 2A, cells present

Table 2. Relative expression of ATM mRNA

No.	Cells	ATM/β-actin
1	Hela	0.76±0.0764
2	Hela^{NC}	0.65±0.0289$^{\#}$
3	Hela^{5746}	0.58±0.1670
4	Hela^{7192}	0.59±0.0702
5	Hela^{4661}	0.45±0.1222
6	Hela^{1057}	0.30±0.1155*

** P<0.05 (Hela^{1057} vs Hela);*
$^{\#}$ P>0.05 (Hela^{NC} vs Hela); n=3.

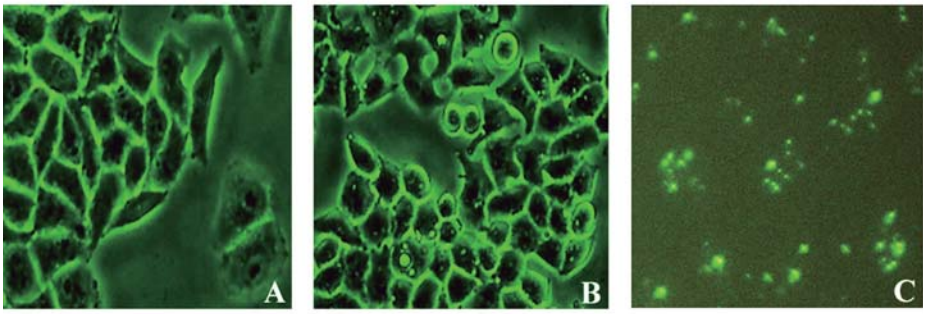

Fig.1 Photos of cells from each group under a fluorescence microscope. A. Hela, B. Hela^{1057}, C. HelaFAM-NC; bright spots in Hela^{1057} with high refractive index, as the mixation of Lipofectamine^{TM}2000 and siRN; C, green fluorescence in cells, as siRNA marked with FAM. Magnification: 10×20.

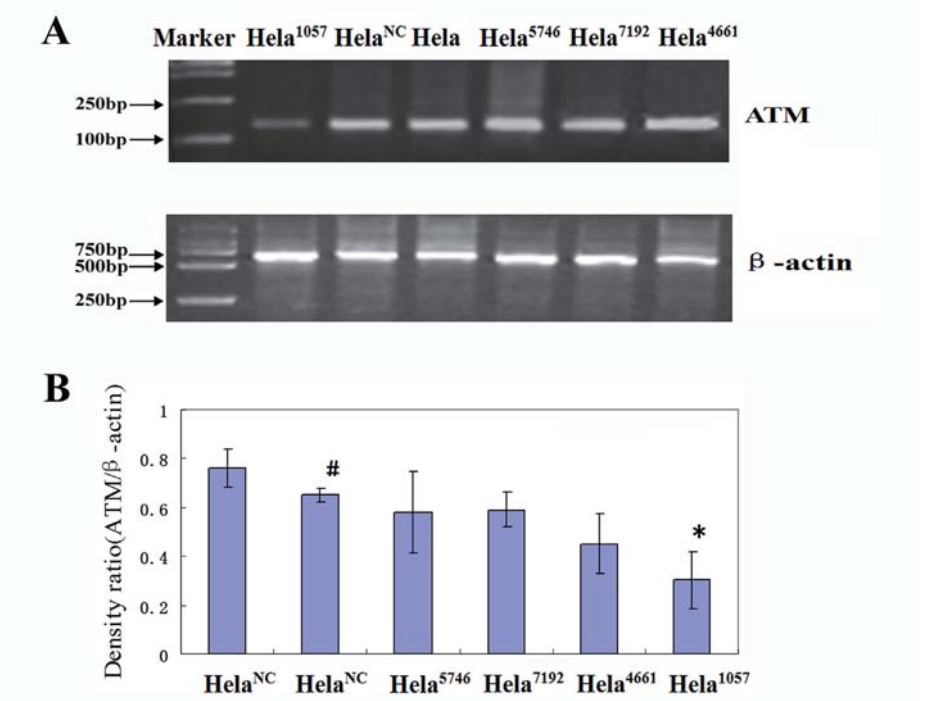

Fig.2 (A) RT-PCR analysis of ATM and β-actin expression at the 24h after the transfection. ATM PCR product 138bp and β-actin PCR product 564bp. (B) Relative Expression of ATM mRNA at 24h after the transfection. Relative expression of ATM cDNA/β-actin cDNA, where *P<0.05 (Hela^{1057} vs Hela), #P>0.05 (Hela^{NC} vs Hela), n=3.

a β-actin target band at 564bp with luminance uniformity, and ATM target band at 138bp with vairous luminance, among which Hela^{1057} is the weakest. As shown in Table 2 and Figure 2B, as for the relative expression of ATM mRNA, Hela cells are the highest, and the relative expression of ATM mRNA of siRNA-transfected Hela^{5746}, Hela^{7192} , Hela^{4661}, Hela^{1057} was reduced to different degrees. Among them, ATM mRNA relative expression of Hela^{1057} was lower than Hela cells (P<0.05), while that od Hela^{5746}, Hela^{7192} and Hela^{4661} did not present significant difference than Hela cells (P>0.05), indicating that 1057-1075nt siRNA has a more intensive interference effect on Hela ATM gene expression. Other siRNA sequences did not present obvios interference effects.

The ATM mRNA relative expression level of Hela^{NC} in the negative control did not present significant difference from Hela (P>0.05), demonstrating that negative control nonspecific nucleic acid sequence can not inhibit the expression of the ATM gene in Hela cells and impose no interference effects. At the same time point, compared with the relative expression of Hela^{1057} and Hela ATM mRNA, significant difference can be observed (P<0.05). Compared with Hela^{NC} and Hela cells, no significant difference can be observed (P>0.05), indicating that 1057-1075nt siRNA can effectively interfere with the ATM gene, and the duration extends to 96h after the transfection with siRNA. As shown in Figure 3A and 3B, in the comparison of Hela^{1057}ATM mRNA at 4 time points, 24h, 48h and 96h after the siRNA transfection present significant difference (P<0.05). Comapred with 96h after the transfection, 72h after the siRNA transfection showed no significant difference (P>0.05), indicating that 1057-1075nt siRNA interfering ATM gene has the optimal effect at 24h and 48h of the transfection, while 72h and 96h showed no significant difference (P>0.05).

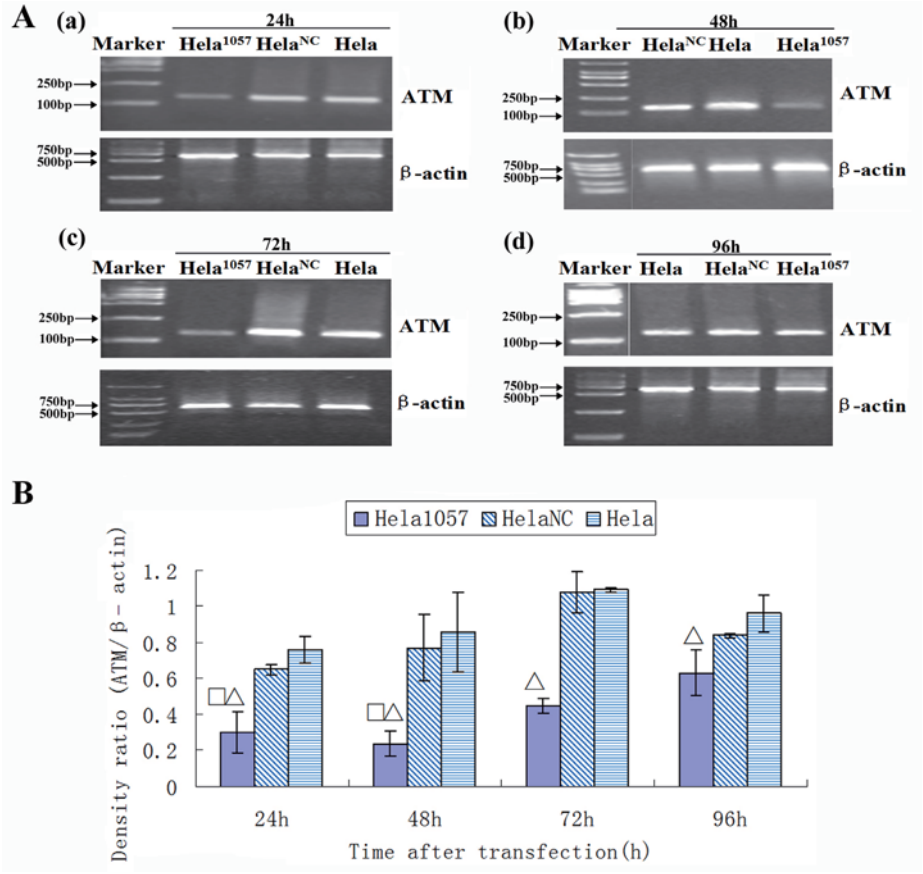

Fig.3 (A) ATM and β-actin RT-PCR electrophoretogram at different time points. (a), (b), (c) and (d) are ATM and β-actin RT-PCR electrophoretogram at 24h, 48h, 72h and 96h after the siRNA transfection. (B) Relative expression of ATM mRNA at different time points. At different time points of 1057-1075nt siRNA transfection of Hela ells, ATM/β-actin relative expression, where ΔP<0.05 (Hela^{1057} vs Hela) , □P<0.05 (Hela^{1057} cell, 24h vs 96h, 48h vs 96h) , n=3.

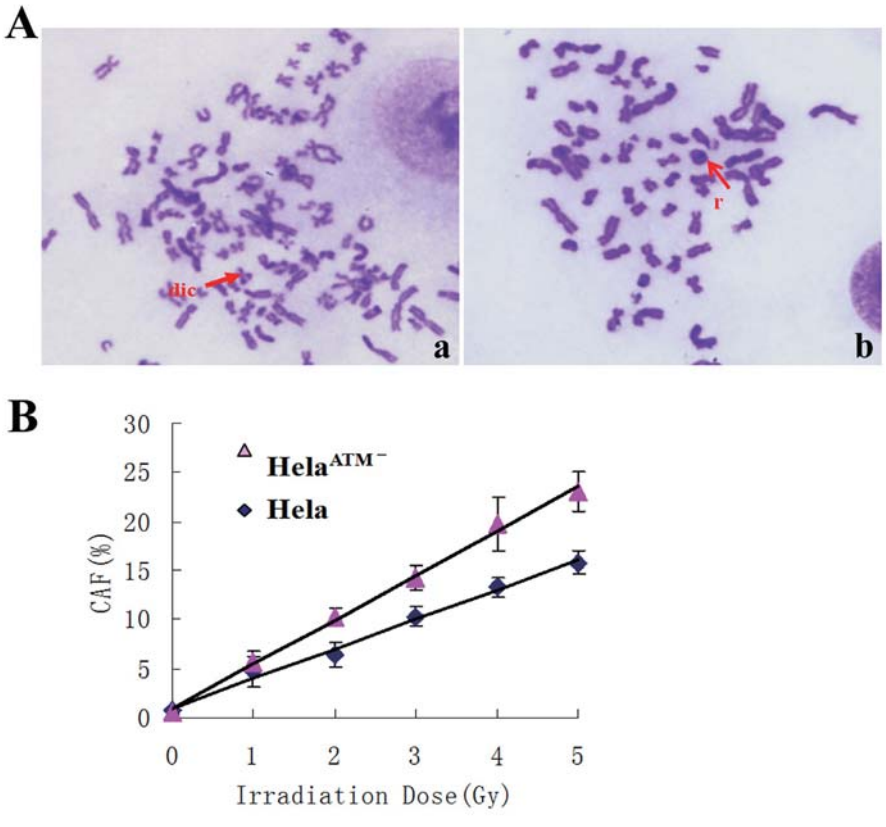

Fig.4 (A) ^{60}Coγ ray-induced Hela and Hela^{ATM-} CA. (a) presents dic, (b) presents r, and the magnification times: 10×100. (B) The relationship between Hela/Hela^{ATM-} CA Rate and the exposure dose (Gy).

2.3 Hela and Hela^{ATM-} Cell Chromosome Aberration Induced by ^{60}Coγ Ray Radiation

In the experimental irradiation dose range, the main type of chromosomal aberrations observed is the dicentric mitochondria. Figure 4A presents the dicentric mitochondria and centromere ring observed under the microscope.

Results of Hela and Hela$^{ATM—}$ cell chromosome aberration induced by ^{60}Coγ ray radiation are shown in Table 3. It can be seen in Table 3 that after the irradiation of 0, 1, 2, 3, 4, and 5Gy ^{60}Coγ ray, the Hela and Hela$^{ATM—}$ cell chromosome aberration increases with rising dosage (P<0.01); except 0Gy, at the same dosage point, aberration rate of Hela$^{ATM—}$ is obviously higher than Hela cells, where 3Gy point showed significant difference (P<0.05), and the difference of the rest dosage showed extreme significance (P<0.01), indicating that after the irradiation, the degree of injury of HelaATM— chromosome cells was more severe than Hela cells and the radiosensitivity of Hela$^{ATM—}$ cells is higher than Hela cells.

2.4 The Relationship between Hela and Hela$^{ATM—}$ CA Rate and the Exposure Dose

Observation results from Table 3 and the correlation analysis showed that Hela and Hela$^{ATM—}$ CA rate is positively correlated with the exposure dose; thus the relationship is shown in Figure 4B and the linear regression equation and the fitting equation are as follows:

Hela$^{ATM—}$ cell chromosome aberration rate: $Y=0.89+4.53D$, $R^2=0.97$, r= 0.98 (P<0.01);

Hela cell chromosome aberration: $Y=1.00+3.01D$, $R^2=0.98$, r= 0.99 (P<0.01).

Where Y is the chromosome aberration rate (%), D is the exposure dose (Gy). It can be seen from the equations that the slope of the linear regression equation of Hela$^{ATM—}$ cell CA rate is significantly greater than Hela cells, presenting significant difference (P<0.05). This indicates that compared with Hela cells, Hela$^{ATM—}$ CA rate grows faster than that of Hela cells along the increase of the dosage.

3 Discussion

ATM gene mutations lead to ataxia-telangiectasia (AT)[8-10], which is a rare autosomal invisible cancer tendency hereditary disease involving the nerves, blood vessels, skin, reticuloendothelial system and endocrine system, clinically presented as progressive cerebellar degeneration, high radiosusceptibility, immunodeficiency, precocious and tumors with high incidence. However, whether ATM expression is associated with chromosome aberration is still not clear.

RNAi extensively exists in advanced plants and animals, as a gene silencing phenomenon mediated by siRNA. RNAi, as an efficient new technology for the specific inhibition of gene expression, has been extensively used in the study of gene function and gene therapy. Theoretically, any genes of human cells can be silenced by RNAi. Commonly used methods to obtain siRNA include chemical synthesis, in vitro transcription, degradation of long fragment of dsRNAs through RNase III, in vitro preparation of siRNA, and cell expression with PCR-prepared siRNA expression cassettes, siRNA expression vector or viral vectors. Each method has advantages and disadvantages, and its application shall take into account the siRNA preparation, difficulty of transfection, the observation of the transfection efficiency, and effect maintaining duration and so on.

Currently, one of the focuses of cancer research is the seeking for sensitizers with high efficiency and low toxicity, that is, to improve the tumor radiotherapy and chemotherapy sensitivity. Among populations, ATM heterozygous carriers account for about 1-2%, their tumor incidence was significantly increased [13]. Vairous studies verified that ATM gene can be used as the potential target for cancer gene therapy [14,15]. In cancer gene therapy, to introduce artificially synthesized siRNA or contructing the siRNA expression vector in tumor cells can specifically inhibit the target gene expression.

In this study, with the chemical synthesis of sequence-specific siRNA for ATM, liposomes were transfected into Hela cells to establish the missing tumor cell model of ATM, thus providing basis for for further study of the tumor radiotherapy and chemotherapy sensitivity. RT-PCR results presented that chemically synthesized siRNA transfected and mediated by liposome entered the Hela cells and successfully inhibited the expression of ATM mRNA (P <0.05). Its interference effects can be continued until 96h after transfection with siRNA, and nonspecific siRNA imposes no impact on ATM mRNA experssion (P<0.05).

The transfection efficiency is an important factor of the experiment, and the transfection method, target gene and cell selection shall be considered. This experiment optimized transfection conditions, and adopted 5ul Lipofectamine^{TM}2000 per pore: 150pmol siRNA transfection of Hela cells (50-60%) presents satisfying effects. In this study, as the transient transfection method is adopted, the long-term maintenance of interference effect of target gene needs to be further explored[16,17]. The application of siRNA in ATM-missing model of other tumor cells, especially radiation-resistant tumor cells (such as glioma cells) should be further studied.

Radiation-induced chromosomal aberrations (CA) make daughter cells after the split unable to obtain a complete set of chromosomes, and die for failing to continue the further splitting. CA is the change of chromosome morphology or structure, and is also a sound index of ionizing radiation damage of cell population, which not only reveals the ionizing radiation damage and evaluates the extent of damage, but also can predict the exposure dosage of personnel under accidents with the established CA dosage-efficiency curve established by the irradiation on in vitro human peripheral blood. Conventional chromosome aberration analysis technique is simple and convenient, thus is used in this study to measure the radiosensitivity of Hela$^{ATM—}$ cells. Various types of

Table 3. CA rate comparison of Hela and Hela$^{ATM—}$ cells after the ^{60}COγ irradiation

dose point Gy	Analysis cell amount	Hela Cells			Hela$^{ATM—}$ Cells		
		dic	r	Total aberration rate (%)	dic	r	Total aberration rate (%)
0	600	4	0	0.67±0.19	4	0	0.67±0.13
1	400	19	0	4.75±1.62**	23	0	5.6±1.15**##
2	200	13	0	6.50±1.35**	19	1	10.0±0.87**##
3	200	20	1	10.5±1.01**	27	1	14.0±1.23**#
4	200	26	0	13.0±2.75**	40	0	20.0±2.75**##
5	200	31	1	16.0±1.21**	45	1	23.0±2.02**##

*** P<0.01, comparison of Hela and Hela$^{ATM—}$ cells at 1, 2, 3, 4, 5Gy with 0Gy;*
 # P<0.05, ## P<0.01, comparison of Hela and Hela$^{ATM—}$ at the same dose point, n=3.

chromosomal aberrations are observed, including the chromosomal pattern aberrations, chromatid aberrations and chromosome amount distortion. The biological dosimetry adopted centromere free ring (r0), dicentric chromosome (dic) and centromere ring (r) and other unstable chromosome aberration frequency to estimate doses. In this study, dic and r are used to calculate the distortion rate of the chromosome.

With conventional chromosome aberration analysis, it is found that after the irradiation with ^{0}Coγ at 0, 1, 2, 3, 4, and 5Gy, CA of Hela and Hela^{ATM-} cells increases with the rising dosage. In addition, at the same dosage point, CA rate of Hela^{ATM-} cells is higher than Hela cells, presenting significant difference ($P<0.01$). This indicates that at the same irradiation dose point, Hela^{ATM-} chromosome damage is greater than Hela cells. For the above materials, according to four kinds of mathematical models provided by WHO ($y=a+bD$, $y=a+bD+cD^2$, $y=kDn$, $y=a+cD^2$) and statistical methods of Wang Jixian and others, curve fitting, regression coefficients and the degree of fitting are tested. $Y=a+bD$ mode is selected as the optimal regression equation. The fitting equation is as follows:

Hela^{ATM-} cell chromosome aberration rate: $Y=0.89+4.53D$, $R^2=0.97$, $r= 0.98$ ($P<0.01$);

Hela cell chromosome aberration: $Y=1.00+3.01D$, $R^2=0.98$, $r= 0.99$ ($P<0.01$).

CA rate of Hela^{ATM-} and Hela cells is positively related with the irradiation dose, and the slope of the linear regression equation of Hela^{ATM-} cell CA rate is significantly greater than Hela cells, presenting significant difference ($P<0.05$). This indicates that compared with Hela cells, Hela^{ATM-} CA rate grows faster than that of Hela cells along the increase of the dosage. The larger the dosage is, the more severe the Hela^{ATM-} chromosome damage is.

After the ionizing radiation of cells, the radiation signals were transduced by the reactive oxygen species (ROS) and DNA strand breaks, which induce the phosphorylation chain reaction of intracellular some columns molecules. Through induction of cell cycle G_1, G_2, and S delay as well as S/M uncoupling mitosis delay, the ionizing radiation influences the cell cycle progression. ATM gene coding protein was involved in cell cycle control, DNA damage signal transduction and repair, stability maintaining and other processes. ATM gene silencing leads to the loss of ATM kinase activity. Ionizing radiation signal failed to activate ATM kinase, thus failing to induce p53 phosphorylation so that p53 regulation was weakened or delayed, and the damaged DNA synthesis was inhibited. This hinders the process of DNA repair, and generates chromosomal instability so that cells became extraordinarily sensitive to the damage factors such as ray, performing features such as enhanced radiosensitivity. In this way, spontaneous CA rate and radiation-induced CA rate became higher than normal cells. These are demonstrated in AT cells with ATM gene mutations [18].

Hela cells are cervical cancer cells transformed by Human Papillomavirus 18 (HPV18). Generally, cervical cancer cell lines contain high gene expressions of HPV E6/E7. The integration of E6 protein, p53 protein, and intracellular E6-associated protein (E6-AP) can promote p53 degradation and its inactivation, so that cells enter S stage from G_1. E7 protein was then integrated with Rb tumor suppressor gene, affecting the integration of Rb and E2F, so that E2F was separated from Rb, entering the gene transcription at S stage. As Hela cells lack G_1 delay, spontaneous CA rate and radiation-induced CA rate became higher. Interfered ATM gene of Hela^{ATM-} cells leads to ATM afunction, also presenting features similar to high radiosensitivity of AT cells, and its radiosensitivity is higher than Hela cells.

In summary, we found that ATM gene was successfully silenced by transfection of chemically synthesized siRNAs in Hela cells, named Hela^{ATM-}. The CAF of Hela^{ATM-} cells was significantly higher than control Hela cells by using conventional chromosome aberration analysis.

Acknowledgements

This work is supported by the National Natural Science Foundation of China (81172597 and 81102078), the Key Programs of Natural Science Foundation of Jiangsu Educational Committee (11KJA310001), Innovative Project for Graduate Students of Jiangsu Province (CXLX11_0082), Scientific Program of Changzhou(CE20125026 and ZD201005) and the Priority Academic Program Development of Jiangsu Higher Education Institutions (PAPD).

References

1. Khanna KK, Lavin MF, Jackson SP, et al. ATM, a central controller of cellular responses to DNA damage . Cell Death and Differentiation ,2001,8(11):1052~65.
2. Gatei M, Scott SP, Filippovitch I ,et al. Role for ATM in DNA damage-induced phosphorylation of BRCA1. Cancer Res,2000,60(12):3299~304.
3. Bender J.A vicious cycle: RNA silencing and DNA methylation in plants. Cell,2001,106(2):129~132.
4. Fire A., Xu S.Q., Montgomery M.K., et al. Potent and specific genetic interference by double-strand RNA in Caenorhabditis elegans. Nature,1998,391(6996):806~811.
5. Elbashir SM., Harborth J. ,Lendeckel W., et al. Duplexes of 21-nucleotide RNAs mediate RNA interference in cultured mammalian cells. Nature,2001,411(6836):494~498.
6. Berns K., Hijmans E.M., Mullenders J.,et al. A large-scale RNAi screen in human cells identifies new components of the P53 pathways. Nature,2004,428(6981):431~437.
7. Tuschl T, Zamore P.D., Lehmann R.,et al. Targeted mRNA degradation by double-stranded RNA in vitro. Genes and Developme nt.,1999,13(24):3191~3197.
8. Gatti RA, Berkel I, Boder E, et al. Localization of an ataxia telangiectasia gene to chromosome 11q22-23. Nature,1988,336(6199):577~580.
9. Savitsky K, Sfez S, Tagle DA, et al. The complete sequence of the coding region of the ATM gene reveals similarity to cell cycle regulators in different species . Humam Molecular .Genetics ,1995,4(11):2025~2032.
10. Uziel T, Savitsky K, Platzer M, et al. Genomic Organization of the ATM gene. Genomics,1996,33(2): 317~320.
11. Lakin ND, Weber P, Stankovic T, et al. Analysis of the ATM protein in wild-type and ataxia telangiectasia cells. Oncogene ,1996,13(12):2707~2716.
12. Cao JP, Meyn MS., Eckardt-Schupp F, et al. TEL1 from Saccharomyces cerevisiae suppresses chromosome aberrations induced by ionizing radiation in Ataxia-telangiectasia cells without affecting cell cycle checkpoint. Radiation and Environmental Biophysics, 2001, 40(4):309~315.
13. Shiloh, Yosef. ATM and related protein kinases :safeguarding genome integrity .Nature Reviews Cancer,2003,3(3):155~168.
14. Collis SJ, Swartz MJ, Nelson WG, et al. Enhanced radiation and chemotherapy mediated cell killing of human cancer cells by small inhibitory RNA silencing of DNA repair factors. Cancer Res,2003,63(7):1550~1554.
15. Chen Shujuan,Wang Gang, G.Mike Makrigiorgos, et al. Stable siRNA-mediated silencing of ATM alters the transcriptional profile of Hela cells. BBRC,2004,317:1037~1044.
16. Chen Zhihong, Vahan B, Indjeian , et al. CP110, a Cell Cycle-Dependent CDK Substrate, Regulates Centrosome Duplication in Human Cells. Dev .Cell,2002,3(3):339~350.
17. Moskalenko S , Henry DO, Rosse c,et al. The exocyst is a Ral effector complex. Nature Cell Biol,2002,4(1):66~72.
18. Kliesch U. Micronucleus test and bone marrow chromosomeanalysis a comparison of methods in vivo for evaluatingchemically induced chromosome alternations. Mutat. Res. 1980;80 : 321.